A modified cross-correlation method for white-light optical fiber extrinsic Fabry-Perot interferometric hydrogen sensors

Zhen Yang*[a,b] , Min Zhang[b] , Yanbiao Liao[b] , Shurong Lai[b] , Qian Tian[a] , Qisheng Li[c] , Yi Zhang[c] , Zhi Zhuang[c]

[a]State Key Laboratory of Precision Measurement Technology and Instruments, Tsinghua University , Beijing China;
[b]Optical Fiber Sensor Lab, Dept. of Electronic Engineering, Tsinghua University, Beijing China;
[c]Institute of Systems Engineering, CAEP, Mianyang, Sichuan China

ABSTRACT

An extrinsic Fabry-Perot interferometric (EFPI) optical fiber hydrogen sensor based on palladium silver (Pd-Ag) film is designed for hydrogen leakage detection. A modified cross correlation signal processing method for an optical fiber EFPI hydrogen sensor is presented.As the applying of a special correlating factor which advises the effect on the fringe visibility of the gap length and wavelength , the cross correlation method has a high accuracy which is insensitive to light source power drift or changes in attenuation in the fiber, and the segment search method is employed to reduce computation and demodulating speed is fast. The Fabry-Perot gap length resolution of better than 0.2nm is achieved in a certain concentration of hydrogen.

Keywords: optical fiber sensor, extrinsic Fabry-Perot interferometer, cross-correlation, fringe visibility

1. INTRODUCTION

Hydrogen as a source of clean, sustainable, and abundant energy is widely used in numerous research and industrial fields. However, hydrogen has the wide explosion range (4–75%), in addition, it easily leaks out due to the smallest molecule size. Therefore, security systems for hydrogen environments require continuous and reliable hydrogen sensors, especially for low concentrations. A number of hydrogen sensors had been proposed and practically applied[1-3]. Many of these sensors involve electrical conductors, limiting their suitability for use in potentially explosive environments[4]. In this paper, we report an EFPI optical fiber hydrogen sensor which has all the advantages of the fiber optic sensors and in addition, it is made immune to source fluctuations, cable and connector losses, and loss of system power. The Fabry–Perot(FP) gap in the EFPI sensor is formed between the endface of a lead-in fiber and a reflector placed at a distance less than a few hundred micrometers to the lead-in fiber endface. The reflections at the lead-in fiber endface and at the reflector are coupled back to the lead-in fiber and interfere to form certain interferometric fringe patterns. The sensing element of this sensor is the Pd-Ag film which is sputtered on the surface of it. We can detect the hydrogen concentration by monitoring the gap length of the EFPI sensor which reflects the stress associated with the hydrogen absorption in the film. The sensor system which is portable and suitable for field detection is formed by a conventional coupler, a low-power LED operating at 850 nm, and a high resolution miniature spectrometer. The interference spectrum which is transferred to a personal computer for further processing is monitored for different concentrations of hydrogen from 0 to 4% in a nitrogen atmosphere. In order to demodulate white light optical fiber EFPI hydrogen sensors with high accuracy and absolute gap length, a modified cross correlation method is presented. The interference spectrum is normalized with the spectrum of the light source. For a low-finesse EFPI sensor, the change of gap length will influence the visibility of the interference fringes reflected back into the fiber. The signal processing method which advises the effect on the fringe visibility has a high accuracy, and the segment search method is employed to reduce computation and demodulating speed is fast. The Fabry-Perot gap length resolution of better than 0.2nm is achieved in 4% hydrogen .

*yyyzzz111@gmail.com; phone 86 10 62781780; fax 86 10 62770317;

2009 International Conference on Optical Instruments and Technology: Advanced Sensor Technologies and Applications, edited by YanBiao Liao, Anbo Wang, Tingyun Wang, Yukihiro Ishii, Proc. of SPIE Vol. 7508, 75081O · © 2009 SPIE
CCC code: 0277-786X/09/$18 · doi: 10.1117/12.839604

2. SENSING PRINCIPLE AND EXPERIMENTAL SET-UP

The basic configuration of our sensor is shown in figure 1.It is fabricated by gluing a silica tube with Pd-Ag film sputtered on it to the lead-in fiber and reflective fiber at both ends. The inner diameter of the silica tube is about 130 um, and the Pd-Ag film thickness is about 100nm. The stress that is induced in the Pd-Ag film during hydrogen absorption depends on the hydrogen concentration. At room temperature, Palladium can absorb up to 900 times its own volume in hydrogen. Exposure to hydrogen converts the palladium to a reversible palladium hydride [5], and the hydrogen content in a Pd-Ag film is a function of the distance away from the outer surface.

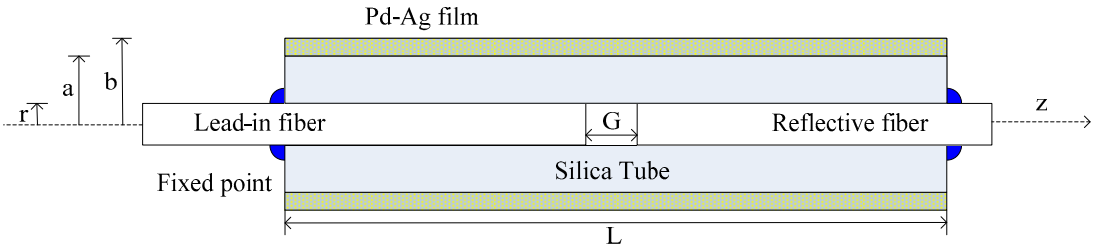

Fig. 1 Schematic diagram of the EFPI hydrogen gas sensor

An EFPI sensor experiences an axial tensile strain when the silica tube with Pd-Ag film expands at the presence of hydrogen. This tensile strain will cause gap length to increase. At equilibrium, the strain of the silica tube is given by

$$\varepsilon_s = \frac{(b^2 - a^2)E_{PA}}{(a^2 - r^2)E_s + (b^2 - a^2)E_{PA}} \cdot \varepsilon_{PA}^{free} \tag{1}$$

where E_{PA} and E_s are the Young's model of Pd-Ag alloy and silica tube respectively, r is the inner radius of the silica tube, a and b are the outer radius of the silica tube and Pd-Ag film respectively, ε_s is the strain of the silica tube and ε_{PA}^{free} is the free strain of the Pd-Ag film at equilibrium.

The ε_{PA}^{free} is experimentally related to the hydrogen content in the alpha phase , and the relationship between hydrogen content and the hydrogen partial pressure follows Sievert's law[6],

$$\varepsilon_{PA}^{free} = \frac{0.026\sqrt{P}}{k} \tag{2}$$

where P is the hydrogen partial pressure (Torr) and k is the Sievert's coefficient (= 350 $Torr^{1/2}$).

The change of the gap length as a function of hydrogen partial pressure can be obtained by using the following expression,

$$\Delta G = \frac{0.026\sqrt{P}}{k}\left[\frac{(b^2 - a^2)E_{PA}L}{(a^2 - r^2)E_s + (b^2 - a^2)E_{PA}}\right] \tag{3}$$

where G is the gap length and L is the length of the silica tube.

The experiment setup for sensor testing is shown in Figure 2. The EFPI sensor was illuminated by a light emitting diode (LED) source around 850 nm through a 2x2 coupler. The interferential light returned from the EFPI was detected by a HR2000+ spectrometer from ocean optics which provides optical resolution as good as 0.035 nm, and the spectrometer was connected to a personal computer via USB port to analyze and store data. The gas supply component consists of a pure hydrogen and pure nitrogen bottle. The gases were mixed together using digital mass flow controllers and connected to the gas cell where the EFPI sensor was located in with nylon piping and connection fittings.

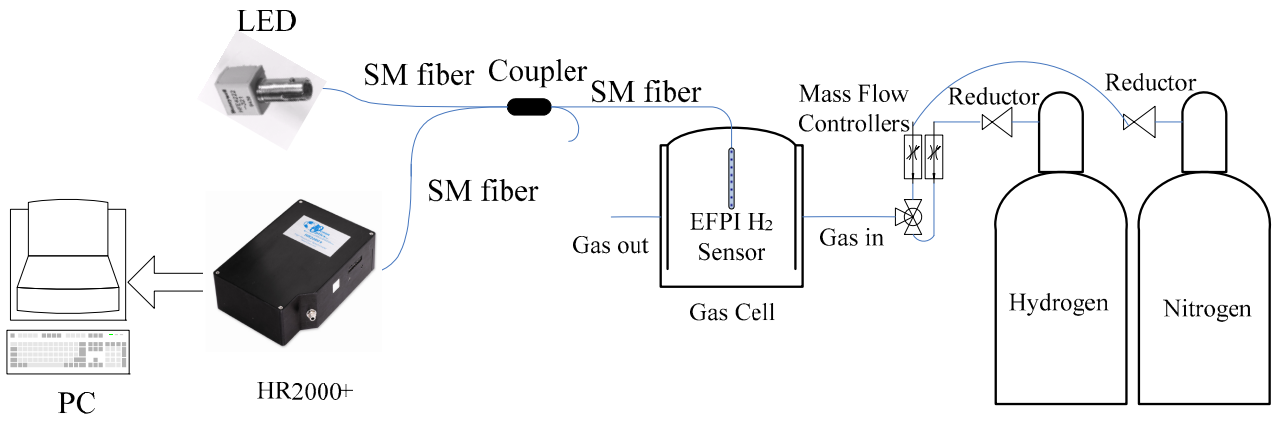

Fig. 2 Schematic of Experimental set-up

3. SIGNAL PROCESSING METHOD

In order to demodulate the EFPI hydrogen sensor with high accuracy, we use a modified cross correlation signal processing method. As the change of gap length will influence the visibility of the interference fringes reflected back into the fiber, it's very necessary to add a special correlating factor.The fringe visibility of a low-finesse gap illuminated by a single-mode optical fiber has been analyzed by modeling of the output of the fiber as a point source [7]. These analyses show that the aperturing effect of the fiber reduces the effective reflection coefficient of the second surface of the gap and is the dominant mechanism for degrading fringe visibility. Here we present an analysis on the fringe visibility of EFPI sensors based on the power distribution.

The FP gap is formed by the end surface of the lead-in fiber and another reflection surface which are perfectly parallel to each other and are perpendicular to the fiber axis *z*. It is assumed that the gap is filled with air.Suppose the fiber has a core radius *a* and is step indexed . The gap length *G* is defined as the distance between the two end surfaces. The reflection coefficients of the interferometer are defined by the weak Fresnel reflections arising from the refractive-index mismatches at the two surfaces of the interferometer and are therefore small.

The guided mode near the core region of a single-mode fiber is approximated very well by a Gaussian function of width w_0 . The Gaussian approximation is suitable for problems involving the field at or near the fiber core but not far from the core. Thus it is suitable for microbending losses that are caused by slight displacements of the core[8].

$$\psi_{e0}(r) = A\exp(-\frac{r^2}{w_0^2}) \tag{4}$$

where *A* is the normalized amplitude, *r* is cylindrical coordinate and w_0 is mode field radius which describes the width of the electric (or magnetic) field distribution. It can be approximated very closely by empirical formula which holds only for step-index fibers[9],

$$w_0 = a(0.65 + \frac{1.619}{V^{1.5}} + \frac{2.879}{V^6}) \tag{5}$$

$$V = (2\pi a/\lambda)NA \tag{6}$$

where *a* is the core diameter of fiber, *V* is the normalized frequency, λ is optical wavelength and *NA* is the numerical aperture of fiber.The complex envelope of the field that emanates from the lead-in fiber and is reflected back to end surface of the lead-in fiber after propagating a length 2*G* in the free space inside the FP gap may be expressed as[10]

$$\psi_{e1}(r,z) = A\frac{w_0}{w_1}\exp(-\frac{r^2}{w_1^2})\exp(-\frac{jk_0r^2}{2R} - j\phi) \tag{7}$$

where $w_1(z) = w_0\sqrt{1+(z/z_R)^2}$ is the mode field radius of the Gaussian beam transmission in free space,

$z_R = \pi w_0^2 / \lambda$ is Rayleigh distance, $k_0 = 2\pi / \lambda$ is the propagation constant, $R(z) = (z^2 + z_R^2)/z$ is the curvature radius of constant phase front and $\phi(z) = -\tan^{-1}(z / z_R)$ is the additional phase shift. The mode-coupling coefficient from ψ_{e0} to ψ_{e1}, which may be expressed as

$$\eta_F = \frac{\iint \psi_{e0} * \psi_{e1} dxdy}{\left(\iint \psi_{e0} * \psi_{e0} dxdy \iint \psi_{e1} * \psi_{e1} dxdy \right)^{1/2}} \tag{8}$$

After the first Fresnel reflection arising from the refractive-index mismatches at the end surface of the lead-in fiber, the reflection intensity can be expressed as

$$I_1 = I_0 R \tag{9}$$

where I_0 is the light source's power spectrum, and *R* is reflectivity.

After the sencend Fresnel reflection at the end surface of the reflective fiber and transmission at the end surface of the lead-in fiber, the intensity of the sencend reflected light can be expressed as

$$I_2 = I_0 (1-R)^2 R \eta_F{}^2 \tag{10}$$

The light propagating along the lead-in fiber is partially reflected by the two end surfaces, and the two reflections are coupled back into the lead-in fiber and interfere to form interferometric fringes.Thus the interference signal can be expressed as

$$\begin{aligned} I_R &= I_1 + I_2 + 2\sqrt{I_1 I_2} \cos\delta \\ &= I_0 R[1 + (1-R)^2 \eta_F{}^2 + 2\eta_F (1-R)\cos\delta] \end{aligned} \tag{11}$$

Where $\delta = \frac{4\pi G}{\lambda} + \pi$ is the phase separation of the interference signal which comprises two terms: the first term is the air gap related phase shift, the second term is the π phase shift that arise from the reflection at the end surface between air and the reflective fiber.

The visibility of the interference spectrum can be expressed as

$$\gamma = \frac{I_{MAX} - I_{MIN}}{I_{MAX} + I_{MIN}} = \frac{2(1-R)\eta_F}{1 + (1-R)^2 \eta_F{}^2} \tag{12}$$

The wavelength and gap length are two factors that influence the visibility in the optical fiber hydrogen sensor system, however, the change of gap length is very small to the visibility. Thus the interference spectrum from the sensor is given by:

$$I(\lambda) = 2 I_S(\lambda)[1 + \gamma \cos\left(\frac{4\pi G}{\lambda} + \pi \right)] \tag{13}$$

where $I_S(\lambda)$ is the spectral power distribution of the LED.

Normalizing (13) with the spectrum of the LED, we can get the normalized interference spectrum which can be expressed as

$$I_n(\lambda) = 2[1 + \gamma \cos\left(\frac{4\pi G}{\lambda} + \pi \right)] \tag{14}$$

Filtering DC items, we can get the simplified form of (14) which can be expressed as

$$I_{nf}(\lambda) = 2\gamma \cos\left(\frac{4\pi G}{\lambda} + \pi\right) \tag{15}$$

Constructing virtual interference spectrum which can be expressed as

$$I_{nv}(\lambda) = 2\gamma' \cos\left(\frac{4\pi G'}{\lambda} + \pi\right) \tag{16}$$

where G' is the virtual gap length and γ' is the corresponding visibility.

Then cross-correlation function can be expressed as[11]

$$\begin{aligned} C(G') &= \int_{\lambda_1}^{\lambda_2} I_{nf}(\lambda) I_{nv}(\lambda) d\lambda \\ &= 4\int_{\lambda_1}^{\lambda_2} \gamma' \cos\left(\frac{4\pi G'}{\lambda} + \pi\right) \gamma \cos\left(\frac{4\pi G}{\lambda} + \pi\right) d\lambda \end{aligned} \tag{17}$$

The cross-correlation function $C(G')$ is maximum when the virtual gap length is equal to the real gap length.

The discrete form of $C(G')$ can be expressed as

$$C(G') = \Delta\lambda \sum_{n=1}^{N} x(n)\gamma'(\lambda_n) \cos\left(\frac{4\pi G'}{\lambda_n} + \pi\right) \tag{18}$$

$$x(n) = \gamma(\lambda_n) \cos\left(\frac{4\pi G}{\lambda_n} + \pi\right) \tag{19}$$

where $x(n)$ is the normalized intensity sequence of the elements of the spectrometer, λ_n is the wavelength corresponding to the element n, and N is the total number of active elements in the spectrometer.

Making G' into equally spaced discrete value within the measurement range, then the cross-correlation function can be expressed as

$$C(G'_m) = \Delta\lambda \sum_{n=1}^{N} x(n)\gamma'(\lambda_n) \cos\left(\frac{4\pi G'_m}{\lambda_n} + \pi\right) \tag{20}$$

where G'_m is the discrete value sequence of gap length within the measurement interval.

As the discrete cross-correlation expression $\gamma'(\lambda_n) \cos\left(\frac{4\pi G'_m}{\lambda_n} + \pi\right)$ is invariable throughout the measurement process, it can be stored in a two-dimensional matrix.

$$fix(m,n) = \gamma'(\lambda_n) \cos\left(\frac{4\pi G'_m}{\lambda_n} + \pi\right) \tag{21}$$

Then discrete cross-correlation calculation is simplified as a two-dimensional matrix and a one-dimensional matrix multiplication process.

$$C(G'_m) = \Delta\lambda \sum_{n=1}^{N} x(n) fix(m,n) \tag{22}$$

To achieve a higher resolution, discrete sequence of gap length has a small interval. Using segment search method could reduce computation and demodulating speed is fast.

4. EXPERIMENTAL RESULTS

The EFPI sensor was detected under normal conditions using the experimental set-up of section 2. Figure 3 shows the gap length change of the EFPI sensor for a thin film of approximately 100nm thick as it was exposed to 4% hydrogen and flushed with 100% nitrogen repeatedly. The plain curve was obtained for increasing hydrogen concentrations starting from 0%. The dotted curve was obtained for decreasing hydrogen concentrations starting from 4%.The sensor showed a reversible response to cycles of hydrogen/nitrogen exposures at low hydrogen concentrations.

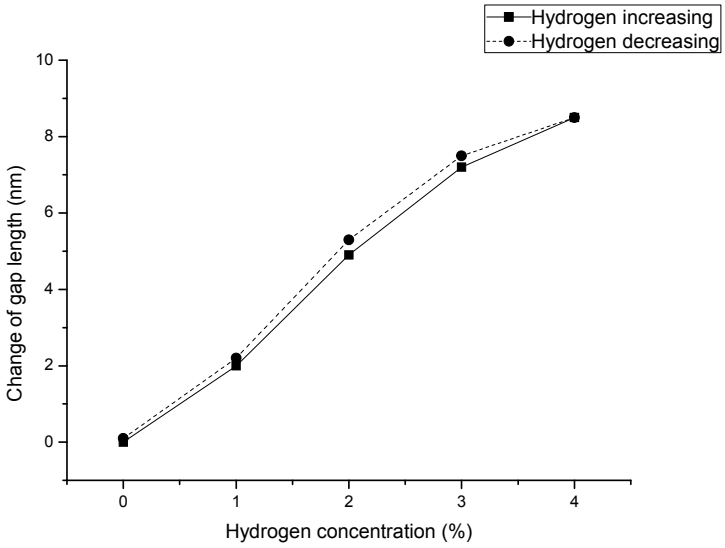

Fig. 3 The gap length change for Hydrogen concentrations from 0% to 4%

Figure 4 shows the hydrogen sensitivities of the EFPI sensors which were exposed to increasing concentrations of hydrogen from 0.2% to 4%. From the figure, the gap length of the sensors increased when the sensor was exposed to a higher hydrogen concentration. The curve (a) in figure 4 shows the gap length change of the sensor with a 50nm thick Pd-Ag film. The curve (b) shows the gap length change of the sensor with a 100nm thick Pd-Ag film.The curves show that the sensitivity improves when the sensor is sputtered with thicker Pd-Ag film and the modified cross-correlation method is suitable for the EFPI optical fiber hydrogen sensors with different thickness of Pd-Ag film.

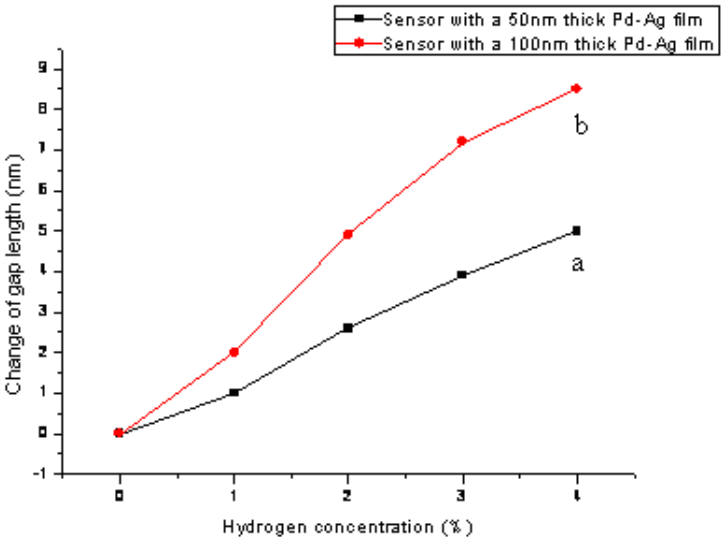

Fig. 4 Hydrogen sensitivities of the EFPI sensors
(a) gap length change of sensor with a 50nm thick Pd-Ag film, (b) gap length change of sensor with a 100nm thick Pd-Ag film

Figure 5 shows the gap length change for Hydrogen concentration at 0%. The fluctuation of the measurement results in Fig.5 is less than 0.4nm which shows that the stability of the sensor is well.

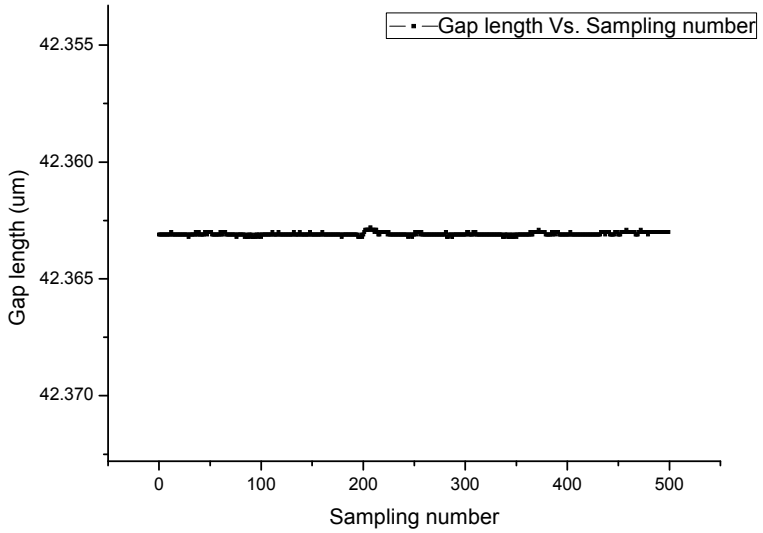

Fig. 5 The gap length change for Hydrogen concentration at 0%

5. CONCLUTION

In summary, we have constructed and demonstrated an EFPI optical fiber hydrogen sensor system which is portable and suitable for field detection. The exposure of the sensor to hydrogen causes the Pd-Ag film to convert to a PdHx film. The PdHx film expands and causes gap length of the sensor changes which can be easily measured by the sensor system. We present an analysis on the fringe visibility of EFPI sensors based on the power distribution. As the applying of a special correlating factor which advises the effect on the fringe visibility of the gap length and wavelength , the cross correlation method has a high accuracy and the method is insensitive to the light source power drift or changes in attenuation in the fiber.

ACKNOWLEDGMENT

This work was supported by National Natural Science Foundation of China and China Academy of Engineering Physics through a grant no: 10776016.

REFERENCES

1. M. A. Butler, "Optical fiber hydrogen sensor," Appl. Phys. Lett., 45, pp. 1007-1009 (1984)
2. M.A. Butler, "Micromirror optical-fiber hydrogen sensor," Sensors andActuators B 22, pp. 155-163 (1994)
3. B.Sutapun, M.Tabib-Azar, and A.A.Kazemi, "Fiber optic Bragg grating sensors for hydrogen gas sensing" Optical Engineering for Sensing and Nanotechnology, Proc. SPIE, Vol. 3740, 278 (1999)
4. M.A. Butler, "Fiber optic sensor for hydrogen concentration near the explosive limit," J. Electrochem. Soc. 138, pp.46-47 (1991)
5. F.A. Lewis, The Palladium Hydrogen System, Academic, New York (1967)
6. M. A. Butler and D. S. Ginley, "Hydrogen sensing with palladium-coated optical fibers," J. Appi. Phys. 64, pp.3706—3711 (1988)
7. Kent A. Murphy, Michael F. Gunther, Ashish M. Vengsarkar, and Richard 0. Claus, “Quadrature phase-shifted, extrinsic Fabry-Perot optical fiber”. Optics Letters, 16(4): 273-275 (1991)

8. Marcuse D. Microdeformation losses of single-mode fibers[J].Appl, Opt. vol. 23, 1084 (1984)
9. Marcuse D. Loss analysis of single-mode fiber splices [J]. Bell Syst.Tech.J，56：703-718 (1977)
10. P. P. Banerjee and T.-C. Poon, Principles of Applied Optics, Irwin, Homewood, Ill (1991)
11. Jing Zhenguo,Yu Qingxu. “White light optical fiber EFPI sensor based on cross-correlation signal processing method.” 6th International Symposium on Test and Measurement, 4: 3509-3511 (2005)